Dual parameter flow cytometry studies in human lymphomas.

S E Shackney, … , T L Lincoln, R J Lukes

J Clin Invest. 1980;66(6):1281-1294. https://doi.org/10.1172/JCI109980.

Research Article

Dual parameter flow cytometry studies using Coulter volume and cell DNA content were carried out in monodisperse cell suspensions of 64 samples of human lymphoma, chronic lymphocytic leukemia, hairy cell leukemia, and benign lymphoid proliferations. Differences in mean Coulter volume among the lymphomas were due both to the intrinsic differences in mean G1 cell Coulter volume and to the presence of increased fractions of larger S and G2 cells, especially among the large B cell lymphomas. However, the relative contribution of large non-G1 cells to the overall population Coulter volume distribution was a relatively minor one; the presence of cells in S did not increase mean Coulter volume by more than 10%, even in samples with high S fractions. There was a good correlation between mean G1 cell Coulter volume and the log of the fraction of cells in S among the B cell lymphomas (r = 0.55). Evidence is presented that within individual samples, large cells proliferate more rapidly than small cells. This was seen in every case, both in the normal samples and in the lymphomas, and in the T cell lymphomas as well as in the B cell lymphomas. Aneuploidy was detected by flow cytometry in 11 cases; in 7 cases the aneuploid cell component could be analyzed separately from the diploid cell component on the basis […]

Dual Parameter Flow Cytometry Studies in Human Lymphomas

STANLEY E. SHACKNEY, KAREN S. SKRAMSTAD, ROBERT E. CUNNINGHAM, DORIS J. DUGAS, THOMAS L. LINCOLN, and ROBERT J. LUKES, *Clinical Pharmacology Branch, Division of Cancer Treatment, National Cancer Institute, Bethesda, Maryland 20205; Department of Pathology, University of Southern California School of Medicine, Los Angeles, California 90033*

ABSTRACT Dual parameter flow cytometry studies using Coulter volume and cell DNA content were carried out in monodisperse cell suspensions of 64 samples of human lymphoma, chronic lymphocytic leukemia, hairy cell leukemia, and benign lymphoid proliferations. Differences in mean Coulter volume among the lymphomas were due both to the intrinsic differences in mean G_1 cell Coulter volume and to the presence of increased fractions of larger S and G_2 cells, especially among the large B cell lymphomas. However, the relative contribution of larger non-G_1 cells to the overall population Coulter volume distribution was a relatively minor one; the presence of cells in S did not increase mean Coulter volume by more than 10%, even in samples with high S fractions. There was a good correlation between mean G_1 cell Coulter volume and the log of the fraction of cells in S among the B cell lymphomas ($r = 0.55$). Evidence is presented that within individual samples, large cells proliferate more rapidly than small cells. This was seen in every case, both in the normal samples and in the lymphomas, and in the T cell lymphomas as well as in the B cell lymphomas. Aneuploidy was detected by flow cytometry in 11 cases; in 7 cases the aneuploid cell component could be analyzed separately from the diploid cell component on the basis of cell Coulter volume differences. The aneuploid components of diploid-aneuploid mixtures had higher S fractions than the diploid components in six of seven cases (0.16 ± 0.04 [SE] vs. 0.08 ± 0.02). These findings are considered in relation to the histopathological classification of the lymphomas, and in relation to the concept of clonal selection and clonal evolution of tumors.

INTRODUCTION

Over the past 15 yr, at least five new histopathologic classification schemes have been proposed for the non-Hodgkin's lymphomas (1). Despite the confusing multiplicity of diagnostic classification systems, there are certain general principles that appear to have general validity. Lymphomas in which large cells are abundant tend to be aggressive clinically (2, 3), and they often respond well to therapy, with relatively high proportions of durable complete remissions (4–6). Small cell lymphomas tend to be less aggressive clinically, but durable complete remissions are infrequent (4, 7).

Predictable relationships between cell size and proliferative behavior might be expected in the lymphomas for at least two reasons.

First, cells increase both in size and in DNA content as they progress through the cell cycle. The dependence of cell size on cell position in the proliferative cycle can be demonstrated in experimental cell systems, by performing paired measurements of electronic cell volume and DNA content on individual cells by means of flow cytometry. This is illustrated in Fig. 1. Thus, the frequencies of large cells in a given lymphoma might be determined by the fractions of large S and G_2 cells.

Second, rapidly proliferating lymphoid cells may be intrinsically larger than slowly proliferating cells. It has been shown that large lymphocytes proliferate more rapidly than small lymphocytes in the normal lymphoid germinal center (8), and in the normal bone marrow (9–11). A relationship between proliferative rate and cell size (which is independent of relative position in the cell cycle) might be preserved in the malignant state as well.

Of course, cell size differences among the lymphomas could also be due to factors that are totally unrelated to their respective proliferative rates or to the presence of different fractions of larger S and G_2 cells.

To study the relationship between cell size and proliferative behavior in the lymphomas, paired cell-by-cell measurements of electronic cell volume

Received for publication 22 April 1980 and in revised form 21 July 1980.

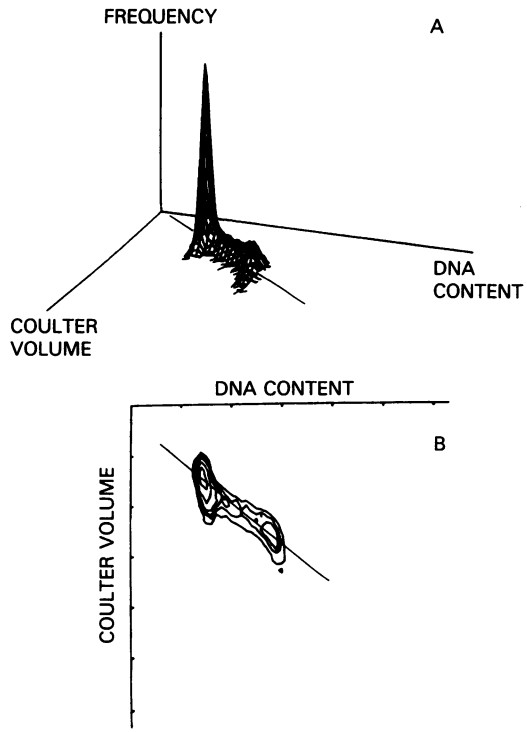

FIGURE 1 (A) The bivariate frequency distributions of Coulter volume and DNA content in mouse sarcoma 180 cells grown in vitro. Small G_1 cells are the most abundant cells in the population. (B) A contour map of the bivariate distribution of Coulter volume and DNA content consisting of horizontal slices through the surface shown in A, viewed from above. It is evident that cells increase in Coulter volume and in DNA content as they progress through the cell cycle, i.e., that they progress along the diagonal line.

and DNA content were obtained in monodisperse cell suspensions of pretherapy biopsy specimens of human lymphoma by means of flow cytometry. Conventional histologic studies and immunologic surface marker studies were done in parallel on the same clinical samples.

METHODS

Clinical samples. The collection and processing of pretherapy biopsy specimens and the techniques for determining immunologic cell surface markers have been described previously (12). Monodisperse cell suspensions were fixed in ethanol for flow cytometry, and stored at 4°C for periods of time ranging from several weeks up to 1 yr. Repeated analyses of individual samples have shown no increase in the coefficient of variation of the DNA content measurement, and no detectable degradation in the electronic cell volume distribution. However, in mithramycin-stained samples, we have noted a hyperchromatic shift in the position of the DNA histogram, the magnitude of which is dependent on the duration of prior storage of ethanol-fixed samples at 4°C (13).

The pertinent data on the clinical samples are summarized in Table I. The majority of the samples were non-Hodgkin's lymphomas. These were grouped by immunologic surface marker characteristics.

The B cell non-Hodgkin's lymphomas were further subdivided into large cell lymphomas, small cell lymphomas, and chronic lymphocytic leukemia (CLL).[1] The large B cell lymphomas include the immunoblastic sarcomas, and large and small noncleaved lymphomas, according to the Lukes and Collins classification (14). These cases were diffuse histiocytic and undifferentiated lymphomas by the Rappaport classification (15). The small B cell non-Hodgkin's lymphomas consisted mostly of cleaved cell lymphomas by the Lukes and Collins classification. These were mostly nodular and diffuse poorly differentiated lymphomas and nodular mixed lymphomas by the Rappaport classification.

The T cell lymphomas included convoluted T cell lymphomas (Lukes and Collins) that would be classified as acute lymphocytic leukemias and diffuse poorly differentiated lymphomas (Rappaport). The small lymphocytic T cell lymphomas (Lukes and Collins) would be classified as well differentiated lymphoma and CLL (Rappaport). The T cell neoplasms also included two thymomas and three cases of Sezary syndrome.

Seven cases of Hodgkin's disease and three cases of hairy cell leukemia were also studied, as were six non-lymphomatous lymph nodes.

Detection of aneuploidy by flow cytometry. Flow cytometry studies were carried out on a Los Alamos Scientific Laboratory cell sorter, and data were recorded, stored, displayed, and analyzed on a Digital Equipment Corp. (Marlboro, Mass.) 11/40 computer using software developed at Los Alamos Scientific Laboratory, Los Alamos, N. Mex. (16). Cell suspensions were stained with mithramycin, and nuclear fluorescence was determined at an excitation wavelength of 457 nm. Between 30,000 and 100,000 cells were analyzed for each sample. DNA content measurements were obtained at constant photomultiplier current. Amplifier gain settings were adjusted so that the mean peak channel or normal human diploid lymphocytes fell in channel 60 on a 256-channel scale. These lymphocytes served as an external biological reference for the diploid host cells that were invariably present in the clinical samples, either alone or admixed with aneuploid cells (13). The problem of mithramycin hyperchromatism (13) is one that cannot be eliminated by mixing reference and sample cells. In the present studies, fixed samples stored for longer than one month were run against external diploid reference standards of comparable fixation age.

In this study, only those samples containing both an endogenous diploid peak and a distinct second peak were considered to contain aneuploid cells. In cases containing unimodal G_1 peaks with high coefficients of variation, it was often possible to identify separate diploid and aneuploid peaks when the samples were rerun (Results). Cases with unimodal G_1 peaks and high coefficients of variation that could not be resolved into separate G_1 peaks were treated as indistinguishable from diploid by flow cytometry in this study.

Determination of the fraction of cells in S phase. The fraction of cells in S phase was calculated by the computer-automated method of Jett (17) in the absence of aneuploidy. In cases where a satisfactory computer fit could not be obtained, and in cases containing overlapping diploid and aneuploid populations, a graphical method developed in our laboratory was used. This graphical method has been shown

[1] *Abbreviation used in this paper*: CLL, chronic lymphotic leukemia.

to give S fraction values that are comparable to the Jett method in cases where both methods could be applied without difficulty. In diploid-aneuploid mixtures that could be resolved either graphically or by dual parameter analysis, S fractions were reported separately for each subpopulation. When a mixture could not be resolved, the S fraction was calculated for the combined population.

Dual parameter studies. Dual parameter flow cytometry studies were performed on each sample. Coulter volume and DNA content were measured for each cell, and the data were stored in the computer cell-by-cell for subsequent analysis.

Coulter volume measurements on ethanol-fixed cells required higher Coulter currents and higher amplifier gain settings than for unfixed cells. In the present studies electronic cell volume measurements were obtained at a current of 1 mA, using a Coulter-type orifice 77 μm Diam. Amplifier gain settings were held constant at a level that was determined on multiple runs to produce values of 35–40 for the mean Coulter volume channel for normal lymphocytes. However, no attempt was made to use the mean Coulter volume of normal lymphocytes as a strict reference standard for each individual clinical sample run. We have reported previously that the Coulter current may degrade the fluorescence signal in dual parameter studies, especially at high amperage and low sample stream flow rates; this effect could be minimized by increasing sample flow rate (18). The dual parameter studies reported here were performed at high sample flow rates, and the Coulter current effects were found to be minimal in nearly all cases. Still, coefficients of variation of the DNA content measurement were often 1–2% higher in the dual parameter studies than in the single parameter studies. Because of this, single parameter DNA content studies were used for the identification and quantitation of aneuploidy and for the S fraction calculation, and dual parameter studies were performed separately on each sample to resolve diploid-aneuploid mixtures and to examine kinetic subpopulations within individual samples.

In samples containing diploid and aneuploid cell populations with overlapping DNA histograms, dual parameter studies were helpful in separating the populations on the basis of differences in Coulter volume. Using computer programs developed by Dr. Gary Salzman (available upon request) at Los Alamos Scientific Laboratory, separate data files for the diploid and aneuploid populations could be generated and each could be analyzed separately, as described in Results. The same computer programs were used to subdivide individual samples into kinetic subpopulations by G_1 Coulter volume. The rationale for this approach is described elsewhere in detail (19, 20). The procedure for subdividing individual samples into component subpopulations is described in Results.

RESULTS

The detection of aneuploidy by flow cytometry. Aneuploidy was found in 11 cases, as shown in Table I. 50% (5/10) of the large B cell lymphomas, 25% (4/16) of the small B cell lymphomas, and 17% (2/12) of the T cell lymphomas were aneuploid. The number of cases is small, however, and the differences are not statistically significant ($P > 0.10$). Hyperdiploid cells were always admixed with diploid cells in varying proportions in the clinical samples. The hyperdiploid cell populations were frequently larger than the admixed diploid cells. In six cases, it was possible to separate the data on the hyperdiploid cells from the diploid cell data on the basis of systematic cell size differences and analyze both sets of data separately.

In one case, a hypodiploid cell population was found admixed with a diploid cell line. The hypodiploid cells differed in size from the diploid cells, and the data for the two populations were separated and analyzed individually.

When data on mixed diploid-aneuploid samples could be resolved into their diploid and aneuploid components, the aneuploid component was taken to represent the lymphoma cell population, since aneuploidy is a reliable marker for identifying neoplastic cells in this setting. The separated aneuploid cases are identified by asterisks in subsequent figures. However, the diploid cells constituted the major component of the sample in most cases and, in all likelihood, many of these diploid cells were also neoplastic.

In these studies, the coefficient of variation of the G_1 peak measurement for normal lymphocytes generally ranged between 3 and 4%. In several lymphoma samples with unimodal diploid G_1 peaks, higher coefficients of variation were observed. In four cases, the coefficient of variation exceeded 4.5% and also exceeded the coefficient of variation obtained with concomitantly analyzed normal lymphocytes by more than 20%. In each of these four cases, a distinct second G_1 peak, whose modal value was 4–6% above the diploid G_1 peak, was identified when the samples were rerun under carefully optimized conditions. These minimally aneuploid G_1 peaks were shown to be present in multiple runs of each sample. In each of these four samples, the aneuploid cell component did not differ sufficiently in Coulter volume from the diploid cell component for the two to be analyzed separately.

When there is a single unimodal diploid G_1 peak, a high coefficient of variation may still indicate the presence of a neoplastic population, as suggested by Barlogie et al. (21) and Diamond and Braylan (22). However, staining artifacts can also produce high coefficients of variation. Since such artifacts may not affect lymphoma cells and reference cells in identical fashion, a comparison with reference cells, either separately or in cell mixing studies, cannot be relied on to eliminate this source of error. Therefore, in this study, samples with single unimodal diploid G_1 peaks and high coefficients of variation were considered indistinguishable from diploid by flow cytometry.

Coulter volume studies. All lymphomas exhibit cytomorphologic heterogeneity to a greater or lesser degree. The large cell lymphomas contain large cells in abundance; large cells are also present in the small cell lymphomas, but their frequency is low.

Differences in mean Coulter volume among the lymphomas could be due to intrinsic cell size differences

TABLE I

Aneuploidy in Relation to Histologic Diagnosis in the Lymphomas

No. of cases	Specimen source	Cytologic type of malignant lymphoma		Ploidy index*
		Lukes and Collins	Rappaport	
B cell lymphomas				
Large B cell lymphomas				
1	Soft tissue	Immunoblastic sarcoma	Diffuse histiocytic	+10%
1	Lymph node	Large noncleaved FCC,‡ diffuse	Diffuse histiocytic	+13%
1	Lymph node	Large noncleaved FCC, diffuse	Diffuse histiocytic	−5%
1	Lymph node	Large noncleaved FCC, diffuse	Diffuse histiocytic	+6%
1	Lymph node	Small noncleaved FCC, diffuse	Diffuse undifferentiated	+4%
1	Lymph node	Small noncleaved FCC, diffuse	Diffuse undifferentiated	Diploid
1	Lymph node	Large noncleaved FCC, follicular	Nodular histiocytic	Diploid
1	Lymph node	Immunoblastic sarcoma	Diffuse histiocytic	Diploid
1	Lymph node	Large noncleaved FCC, diffuse	Diffuse histiocytic	Diploid
1	Spleen	Large noncleaved FCC, diffuse	Diffuse histiocytic	Diploid
Small B cell lymphomas				
1	Lymph node	Small cleaved FCC, follicular	Nodular poorly differentiated	+15%
1	Spleen	Small cleaved FCC, follicular	Nodular poorly differentiated	+77%
1	Lymph node	Small cleaved FCC, follicular	Nodular poorly differentiated	+5%
1	Soft tissue	Small cleaved FCC, follicular	Nodular poorly differentiated	+5%
1	Lymph node	Small cleaved FCC follicular	Nodular mixed	Diploid
1	Spleen	Small cleaved FCC, diffuse	Diffuse poorly differentiated	Diploid
3	Lymph node	Small cleaved FCC, follicular	Nodular poorly differentiated	Diploid
1	Spleen	Small cleaved FCC, follicular	Nodular poorly differentiated	Diploid
1	Lymph node	Small cleaved FCC, diffuse	Diffuse poorly differentiated	Diploid
1	Lymph node	Large cleaved FCC, follicular	Nodular poorly differentiated	Diploid
1	Lymph node	Large cleaved FCC, diffuse	Diffuse poorly differentiated	Diploid

TABLE I (*Continued*)

No. of cases	Specimen source	Cytologic type of malignant lymphoma		Ploidy index*
		Lukes and Collins	Rappaport	
1	Soft tissue	Large cleaved FCC, follicular	Nodular histiocytic	Diploid
1	Peripheral blood	Aggressive CLL	CLL	Diploid
CLL				
1	Spleen		CLL	Diploid
9	Peripheral blood		CLL	Diploid
T cell lymphomas and thymomas				
1	Pleural fluid	Convoluted T cell lymphoma	Acute lymphocytic leukemia	+62%
1	Spleen	Convoluted T cell lymphoma	Diffuse poorly differentiated lymphoma	+12%
1	Pleural fluid	Convoluted T cell lymphoma	Diffuse poorly differentiated lymphoma	Diploid
1	Peripheral blood	Convoluted T cell lymphoma/leukemia	Diffuse poorly differentiated lymphoma	Diploid
1	Bone marrow	Convoluted T cell lymphoma/leukemia	Acute lymphocytic leukemia	Diploid
1	Lymph node	Small lymphocytic T cell lymphoma	Diffuse well differentiated lymphocytic lymphoma	Diploid
1	Peripheral blood	C (T cell) LL	CLL	Diploid
1	Lymph node	Thymoma		Diploid
1	Peripheral blood	Thymoma		Diploid
3	Peripheral blood	Sezary syndrome		Diploid
		Histologic subtype		
Hodgkin's disease				
2	Spleen	Lymphocyte depleted Hodgkin's disease		Diploid
2	Lymph node	Mixed cellularity Hodgkin's disease		Diploid
1	Lymph node	Lymphocyte predominance Hodgkin's disease		Diploid
1	Lymph node	Nodular sclerosing Hodgkin's disease		Diploid
1	Spleen	Nodular sclerosing Hodgkin's disease		Diploid
Hairy cell leukemia				
2	Spleen	Hairy cell leukemia		Diploid
1	Peripheral blood	Hairy cell leukemia		Diploid
Nonlymphomatous states				
3	Lymph node	Reactive follicular hyperplasia		Diploid
1	Lymph node	Reactive follicular and interfollicular hyperplasia		Diploid
1	Spleen	Granulomatous process		Diploid
1	Spleen	Reactive hyperplasia		Diploid

* Ploidy index is defined as $100 \times \left(\frac{\text{sample mean [or modal] } G_1 \text{ channel}}{\text{external reference mean } G_1 \text{ channel}} - 1\right)$.

‡ FCC, follicular center cell.

that are unrelated to cell position in the cell cycle. On the other hand, it is possible that different lymphomas may have comparable G_1 cell Coulter volumes but may differ in overall population mean Coulter volume because of differing proportions of larger S and G_2 cells. In the examples shown in Fig. 2, it is apparent that both factors may be important. In case A (Fig. $2A_1$ and $2A_2$), the exclusion of a relatively large fraction of non-G_1 cells reduced mean population Coulter volume by ~15%. In case B (Fig. $2B_1$ and $2B_2$), the fraction of non-G_1 cells is quite small, and its contribution to the Coulter volume distribution is negligible. However, the mean Coulter volume of the G_1 cells in case A is still 20% greater than the mean Coulter volume of G_1 cells in case B, indicating that there are also intrinsic size differences between the two samples that are unrelated to cell position in the proliferative cycle.

As these two cases show, intrinsic differences in cell size among the lymphomas can be assessed separately from cell cycle position-dependent differences in cell size by comparing the Coulter volume distributions of the G_1 cells only among different samples. The results are shown in Fig. 3. Overall, the G_1 cells in the large B cell lymphomas were larger than the G_1 cells of the small B cell lymphomas, and these, in turn, were larger than the G_1 cells in CLL. There was considerable overlap in G_1 cell Coulter volumes among the groups, but the differences among the means for the B cell groups (including CLL) were statistically significant ($P < 0.05$). The mean Coulter volume of G_1 lymphocytes from reactive lymph nodes and from lymph nodes with Hodgkin's disease were indistinguishable from those of normal lymphocytes circulating in the peripheral blood. The G_1 cells of hairy cell leukemia were larger than those of normal lymphocytes, but the number of cases was too small for statistical evaluation. Overall, the flow cytometric measurements of Coulter volume were in general agreement with qualitative observations by light microscopy, and with the Coulter volume studies of Braylan et al. in the lymphomas (22, 23).

The separation of data in diploid-aneuploid cell mixtures. The separation of the diploid and aneuploid cell population data by means of dual parameter analysis is exemplified by the case shown in Fig. 4. The DNA content distribution is shown separately in Fig. 4A. There is a diploid G_1 peak, a hyperdiploid G_1 peak, overlapping diploid and aneuploid S regions, a tetraploid G_2M peak, and a hypertetraploid G_2M peak. The Coulter volume distribution is shown separately in Fig. 4B. There are at least two populations whose Coulter volumes overlap. The bivariate distribution, illustrated in Fig. 4C, shows that all of the aneuploid

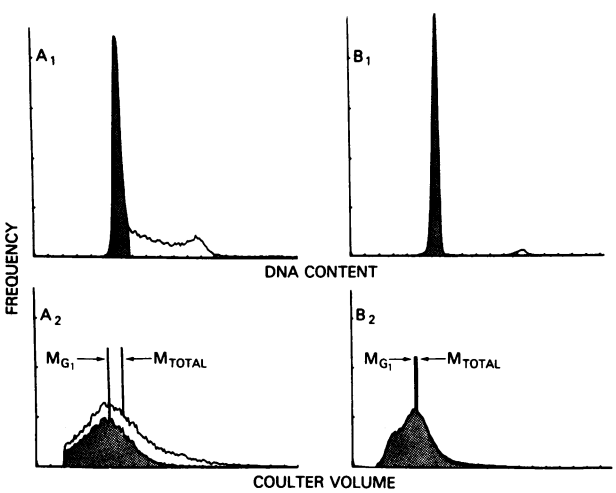

FIGURE 2 (A) Comparison of the relative contributions to the observed Coulter volume distribution of intrinsic G_1 cell Coulter volume and the presence of larger S and G_2 cells in two cases. (A_1) The DNA content distribution in A exhibits a large fraction of non-G_1 cells (unshaded region). The G_1 cell population (shaded region) includes some cells in early S due to overlap of G_1 and S regions. Debris and cell fragments in the pre-G_1 region are excluded from the analysis. (A_2) For case A, the mean (M_{G_1}) of the Coulter volume distribution of the G_1 cells (shaded region) is in channel 52. The mean (M_{Total}) of the total cell population is in channel 61. Non-G_1 cells (unshaded region) are found throughout the distribution, but are the predominant component among the large cells. (B_1) Case B is composed almost entirely of G_1 cells (shaded region). (B_2) In case B, the Coulter volume distribution of the G_1 cells (shaded region) represents nearly all of the cells. The contribution of the non-G_1 cells is negligible, so that M_{G_1} is in channel 43 and M_{Total} is in channel 44. Note that M_{G_1} for case A is higher than M_{G_1} for case B. For discussion see text.

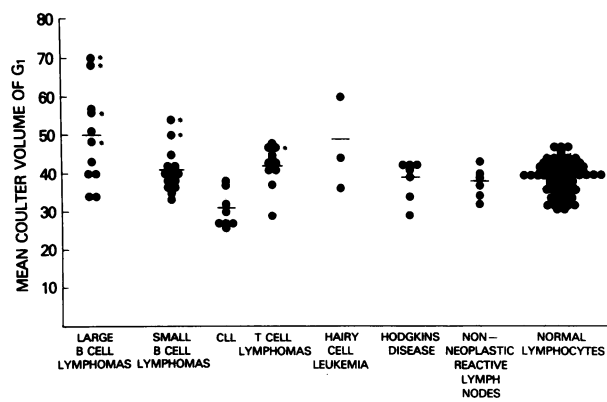

FIGURE 3 Mean Coulter volume channel number of G_1 cells for various lymphoid cell populations. Asterisks identify aneuploid component of separated diploid-aneuploid mixtures. Group means shown by horizontal bars. Large B cell lymphomas, mean G_1 channel number 50±4 (SE); small B cell lymphomas, 40.6±1.41; CLL, 30.5±1.5; T cell lymphomas, 42±1.6; hairy cell leukemia, 48±5.8; Hodgkin's disease, 37.7±1.5; reactive nodes, 37.5±1.6, normal lymphocytes, 39.3±0.5. For discussion, see text.

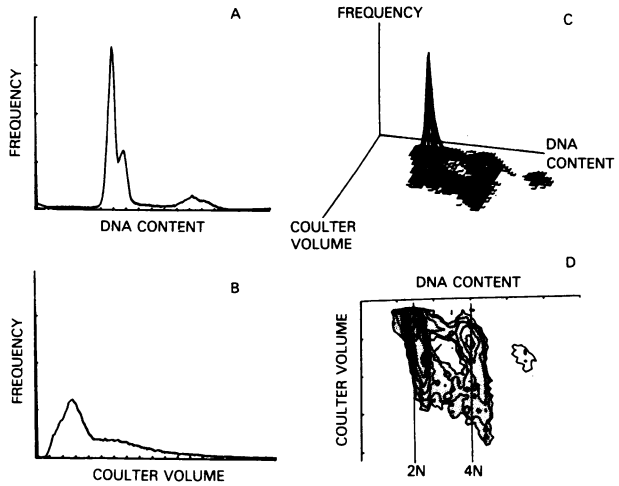

FIGURE 4 Single and dual parameter studies in a lymphoma sample containing a mixture of diploid and aneuploid cells. (A) The DNA content distribution. (B) The Coulter volume distribution. (C) Bivariate distribution of Coulter volume and DNA content. (D) Contour map of the bivariate distribution, consisting of multiple horizontal slices through the surface shown in A, viewed from above. 2N and 4N lines represent diploid and tetraploid reference lines, respectively. For discussion, see text.

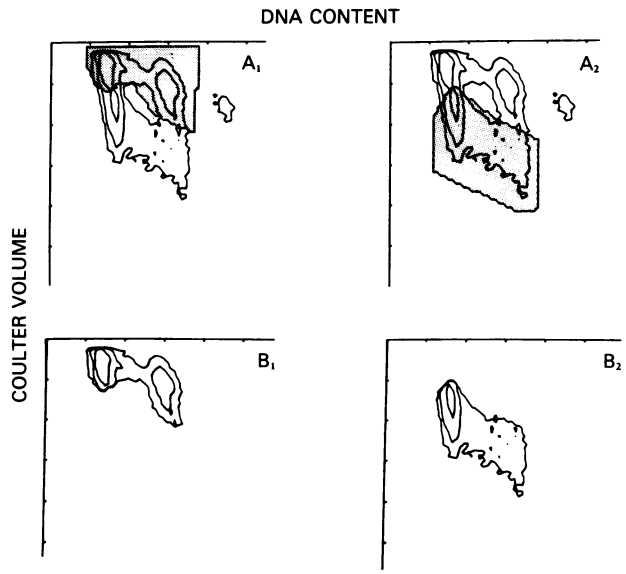

FIGURE 5 The separation of diploid and aneuploid components from a mixture by dual parameter analysis. (A_1) Computer-assisted enclosure of smaller diploid population within a bounded region (shaded area). (A_2) Computer-assisted enclosure of larger aneuploid population within a separate bounded region (shaded area). (B_1 and B_2) Contour maps of separate files of the small diploid and large aneuploid populations, respectively.

cells are much larger than all of the diploid cells at every stage of the cell cycle. This is made clear in Fig. 4D, which is a contour map of the surface in Fig. 4C. The contour map shows a diploid G_1 "spot" connected to a tetraploid G_2M spot by a bridge in the S region, and a separate spot of large hyperdiploid cells, connected by a bridge of large aneuploid S cells to a diffuse spot of very large hypertetraploid cells.

With the aid of the computer, it was possible to enclose the diploid and hyperdiploid populations within separate bounded regions (shaded areas, Figs. $5A_1$ and $5A_2$). The data on cells falling within each region were stored in separate files (Figs. $5B_1$, and $5B_2$) that could then be analyzed individually. The relative contributions of the separated cell populations to the original mixture are shown in Fig. 6. It is apparent that the population mixture was comprised largely of diploid cells (Fig. $6A_2$) with small Coulter volumes (Fig. $6B_2$). Those diploid cells found in later stages of the cell cycle were larger, producing the tail of the shaded region in Fig. $6A_2$. The aneuploid cells were a minor component of the mixture (Fig. $6B_3$) but made up the majority of the large cells in the Coulter volume distribution (Fig. $6A_3$).

In 7 of the 11 cases exhibiting aneuploidy, the aneuploid component was separable from the diploid component. Among the large B cell lymphomas with separable aneuploid populations, the aneuploid cell fraction in each sample ranged from 27 to 54% of the total; in the two small B cell lymphomas and in the T cell lymphoma with separable aneuploid populations, the aneuploid cell fraction in each sample ranged between 10 and 12% of the total.

The fraction of cells in S and its relation to population mean Coulter volume. The fraction of cells in S for the various groups are shown in Fig. 7. The highest S fractions were found among the large B cell lymphomas; the differences in S fraction between the large and small B cell lymphomas were statistically significant ($P < 0.01$).

In six of the seven cases with separable diploid and aneuploid components, the S fraction of the aneuploid cell population was higher than the S fraction of the diploid cell population in the same sample, with a mean of 0.16 ± 0.04 (SE) for the aneuploid component and a mean of 0.08 ± 0.2 for the diploid component. The differences in S fraction between the aneuploid and diploid component in each sample were statistically significant ($P < 0.05$).

The mean S fraction of the diploid cells in the separable diploid-aneuploid mixed samples was higher than that of lymphocytes in non-neoplastic reactive lymph nodes (Fig. 7). The difference was not statistically significant.

The diploid cell component of the lymphomatous nodes may have consisted of normal host lymphocytes that were stimulated to proliferate rapidly in the presence of the aneuploid lymphoma cells, or they

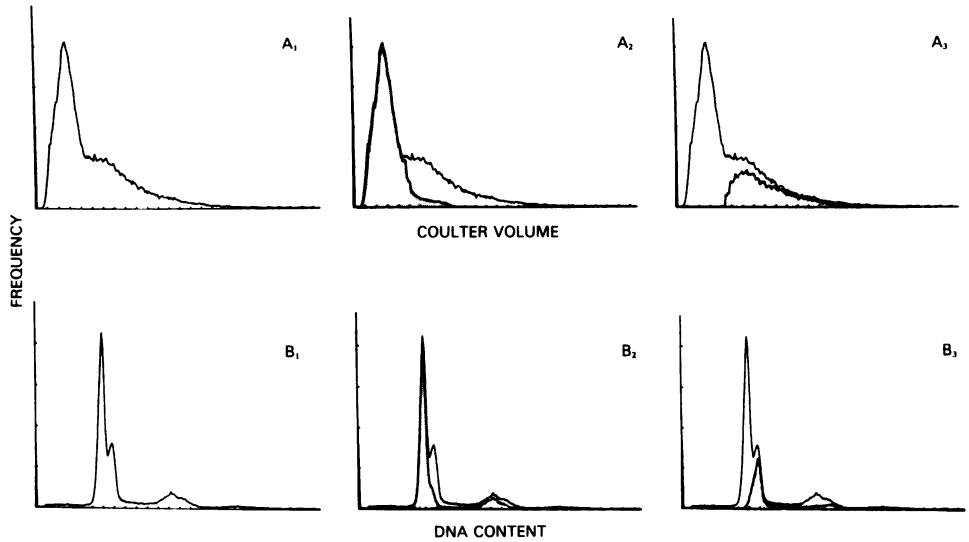

FIGURE 6 The relative contributions of the small diploid and large aneuploid populations shown in Fig. 5 to the overall Coulter volume and DNA content distributions. (A_1) The combined Coulter volume distribution. (B_1) The combined DNA content distribution. (A_2) The contribution of the small diploid population (shaded region) to the combined Coulter volume distribution. (B_2) The contribution of the small diploid population to the combined DNA content distribution. There is still some residual contamination by aneuploid cells, as evidenced by the small shoulder on the descending limb of the G_1 peak. (A_3) The contribution of the large aneuploid population to the combined Coulter volume distribution. (B_3) The contribution of the aneuploid population to the DNA content distribution. Note that there is still some residual contamination by diploid cells, as evidenced by the more gradual upstroke of the ascending limb of the G_1 peak. For further discussion, see text.

may have contained separate neoplastic stem lines with DNA contents indistinguishable from the normal diploid by flow cytometry. The latter possibility is the more likely, because histologically each of these nodes was largely replaced by neoplastic cells.

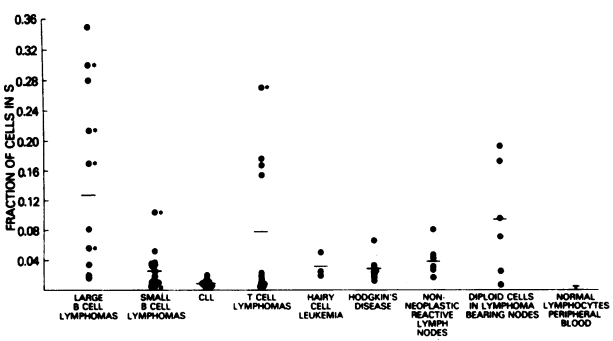

FIGURE 7 The fraction of cells in S for different groups of lymphoid cell populations. Asterisks identify the aneuploid component in separated diploid-aneuploid mixtures. Horizontal bars represent group means. Large B cell lymphomas, mean S fraction 0.13±0.04 (SE); small B cell lymphoma, 0.025±0.006; CLL, 0.008±0.001; T cell lymphomas, 0.06±0.02; hairy cell leukemia, 0.02±0.008; Hodgkin's disease, 0.027±0.007; reactive lymph nodes, 0.07±0.02; diploid cells in lymphomatous nodes, 0.08±0.02; normal lymphocytes, <0.005. For discussion, see text.

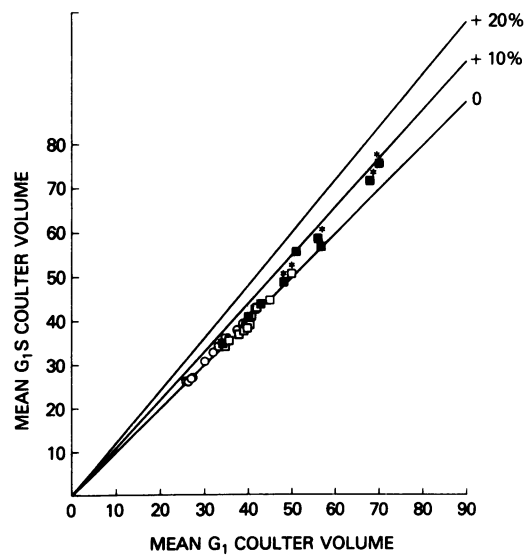

FIGURE 8 B cell lymphomas. The relative contribution of mean G_1 Coulter volume and of the Coulter volumes of larger S cells to overall population mean Coulter volume among the B cell lymphomas. Ordinate: mean G_1S Coulter volume channel number. Abscissa: mean Coulter volume channel number of G_1 cells only. The added contribution to mean Coulter volume of cells in S would elevate the position of a given sample point above the diagonal labeled zero. ■, Large B cell lymphomas; □, small B cell lymphomas; ○, CLL.

To assess the relative contribution of large S cells to the overall Coulter volume distribution in the B cell lymphomas, the mean Coulter volume of G_1 + S cells is plotted against the mean Coulter volume of the G_1 cells alone for each sample in Fig. 8. It is apparent that the observed differences in mean Coulter volume among the lymphomas are attributable largely to differences in the Coulter volumes of the G_1 cells. The contribution of S cells to the overall population Coulter volume distribution was relatively small in all cases. The inclusion of S cells did not increase mean population Coulter volume by more than 10% in any sample, and then only among the large B cell lymphomas.

It is apparent from Fig. 9 that there is a correlation between mean G_1 Coulter volume and S fraction among the B cell lymphomas. Five of six B cell lymphomas with mean G_1 Coulter volume channel numbers >50 had S fractions >0.08. None of the cases with mean G_1 Coulter volume channel numbers <50 had S fractions >0.08. The correlation coefficient between mean G_1 Coulter volume and the logarithm of the S fraction in the B cell lymphomas was 0.55. This correlation underscores the relationship between large cell size and rapid growth rate in the B cell lymphomas.

In contrast, there is no apparent correlation between mean G_1 Coulter volume and the S fraction among the T cell lymphomas.

Analysis of kinetic subpopulations within individual samples. The same technique of computer-implemented data sorting that was used to separate the data of diploid cells from aneuploid cells in diploid-aneuploid mixtures could also be used to examine kinetic subpopulations of uniform ploidy within individual samples. In order to perform such analyses, we relied on the principle illustrated in Fig. 1 that proliferating cells move along diagonal pathways on the bivariate Coulter volume-DNA content plane. That is, it was assumed that the small G_1 cells increase in size as they proceed through the cell cycle to produce the small G_2 cells of the population (cut 1, Fig. $10A_2$); similarly, it was assumed that the large G_1 cells increase in size as they progress through the cycle to produce the large G_2 cells (cut 6, Fig. $10A_2$). Frames B_2-B_7 in Fig. 10 confirm that the range of Coulter volumes increases progressively with successive cuts. Frames C_2–C_7 in Fig. 10 show that the fraction of cells in S increases progressively in cuts with progressively larger G_1 Coulter volumes.

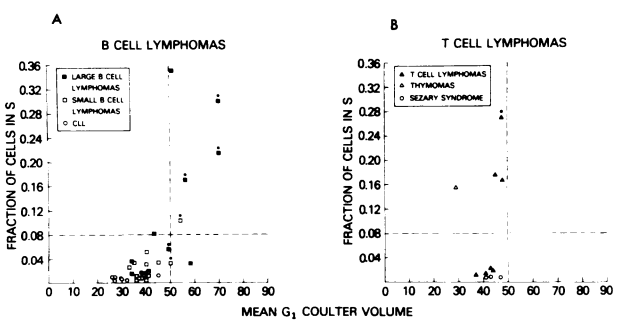

FIGURE 9 The relation between mean G_1 Coulter volume and fraction of cells in S among the B cell lymphomas (A), and among the T cell lymphomas (B) For discussion, see text.

When this diagonal strip analysis technique was applied to the reactive lymph node samples in our series, it was apparent that the subpopulations with the largest mean G_1 Coulter volumes within each lymph node also had the highest S fractions, as shown in Fig. 11. These findings essentially confirm the experimental observations that the large lymphoid cells in the dark zone of the normal lymph node germinal center exhibit a higher [^{3}H]thymidine pulse labeling index than the smaller lymphocytes found in the light zone (8).

The same fundamental relationship between mean G_1 Coulter volume and fraction of cells in S was found to hold true for cell subpopulations within each sample in all of the lymphoma samples that could be subjected to the diagonal strip analysis technique. The results are shown in Fig. 12. The data for the case illustrated in Fig. 10 are represented by the dotted line in Fig. 12A. Similar results were obtained in the other large B cell lymphomas (Fig. 12A), in the T-cell lymphomas (Fig. 12B), in the small B cell lymphomas (Fig. 12C), and in Hodgkin's disease (Fig. 12D).

In each of the cases shown in Figs. 11 and 12, the angles for the strips were determined from the slope of the line connecting the high point of the G_1 peak with the high point of the G_2 peak of the bivariate distribution. When the G_2 peak was very low or diffuse, the slope of the ridge of cells in S was used. The effects of varying the angle of the strips were examined separately in each case. Over a range of angles spanning ~40–80 degrees with respect to the Coulter volume axis, there were only minor changes in the S fractions in individual strips, and the relationship of increasing S fraction with increasing G_1 Coulter volume was always preserved. Thus, in each clinical sample, the frequency of large cells in S was high in relation to the overall frequency of large cells, and the frequency of small cells in S was low in relation to the overall frequency of small cells, regardless of how the data were partitioned, within reasonable bounds. The advantage of using narrow diagonal strips to partition the data is that this technique is based on sound biological principles (Fig. 1 and associated discussion); this technique demonstrates the gradual nature of the change in S fraction with changing G_1 Coulter volume.

Thus, the correlation between mean G_1 cell Coulter volume and S fraction holds not only among different B cell lymphoma samples, but among different kinetic

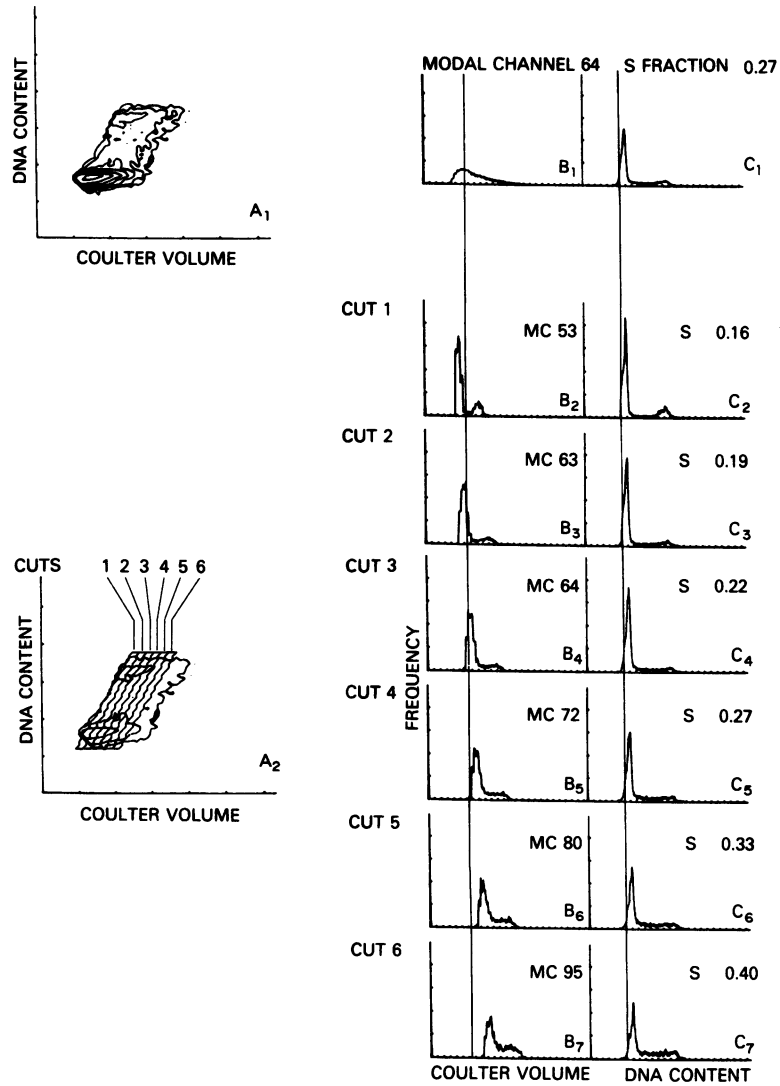

FIGURE 10 The partition of an aneuploid population that is homogeneous with respect to ploidy into kinetic subpopulations by G_1 Coulter volume. (A_1) A contour map of the bivariate distribution of the overall aneuploid population, as in Fig. $5B_2$. (B_1) The Coulter volume distribution of the overall aneuploid population, as in Fig. $6A_3$. The modal channel is 64. (C_1) The DNA content distribution of the overall aneuploid population, as in Fig. $6B_3$. The fraction of cells in S is 0.27. (A_2) The partition of the population by diagonal cuts or strips (for explanation, see text). (B_2–B_7) The modal channel for G_1 cells (MC) increased from 53 in cut 1 to 95 in cut 6. (C_2–C_7) The fraction of cells in S increased progressively from 0.16 in cut 1 to 0.40 in cut 6.

subpopulations within each sample. It is of interest that this correlation is demonstrable among subpopulations within each T cell lymphoma sample, but not among different T-cell lymphomas (Fig. 9).

DISCUSSION

The present studies demonstrate that multiparameter flow cytometry can be used to perform quantitative histopathologic analyses in human lymphomas. Paired cell-by-cell measurements of Coulter volume and DNA content can be used to separate aneuploid cell data from diploid cell data in diploid-aneuploid cell population mixtures.

Populations that are homogeneous with respect to ploidy by flow cytometry still exhibit a considerable degree of heterogeneity with respect to cell Coulter volume. It is clear that there are correlations between Coulter volume and cell DNA content that are valid both among tumor samples and among subpopulations within individual tumor samples. Principles that govern the dynamic behavior of proliferat-

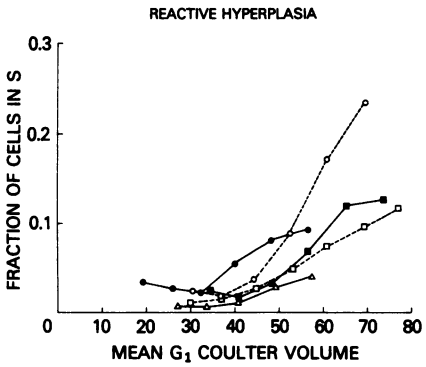

FIGURE 11 The relation between mean G_1 Coulter volume and the fraction of cells in S in cell subpopulations, obtained by the diagonal strip method shown in Fig. 10, within individual samples of non-neoplastic reactive lymph nodes. Each curve represents a separate sample. The points on each curve represent data from consecutive diagonal strips within each sample. Fraction of cells in S for each strip is plotted on the ordinate against mean G_1 Coulter volume channel number on the abscissa.

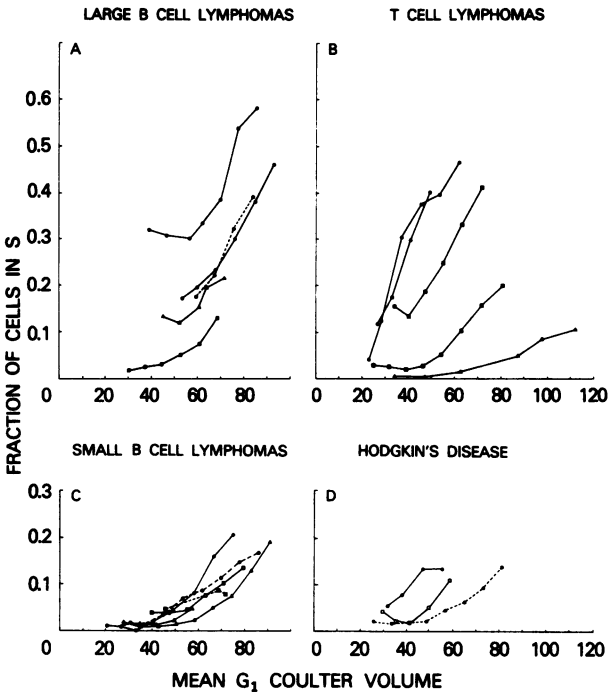

FIGURE 12 The relation between mean G_1 Coulter volume and the fraction of cells in S in cell subpopulations, obtained by the diagonal strip method shown in Fig. 10, within individual samples of lymphoma. Each curve represents a separate sample. The points on each curve represent data from consecutive diagonal strips within each sample. Fraction of cells in S is plotted on the ordinate against mean G_1. Coulter volume for each strip is plotted on the ordinate against mean G_1 Coulter volume channel number on the abscissa. (A) Large B cell lymphomas. (B) T cell lymphomas. (C) Small B cell lymphomas. (D) Hodgkin's disease.

ing cell populations in general, and the growth behavior of cells of the reticuloendothelial system in particular, can be brought to bear to understand these relationships.

The microarchitectural organization of mammalian tissues into separate regions of rapid and slow cell proliferation, with cell migration from the former to the latter over the course of time is well documented in a variety of normal tissues (24–37) and in experimental tumors (38). In the normal lymphoid germinal center and in the normal bone marrow, cell migration and growth retardation are accompanied by a clearly demonstrable morphologic transition from large to small cell size. Similar differences in the proliferative rates of large and small malignant cells have been found repeatedly both in human leukemia (39–43) and in experimental mouse lymphoma/leukemia (44, 45). In several studies, the transition from rapidly proliferating large leukemic cells to slowly proliferating or nonproliferating small leukemic cells has been documented (40–42, 44, 45).

The studies reported here suggest that the short-term cytomorphologic transitions that accompany growth retardation in the normal lymphoid germinal center and bone marrow and in the leukemias may also occur in human lymphomas under near steady-state conditions.

Our findings in the lymphomas are consistent with the model shown in Fig. 13. The model consists of the following elements: (*a*) It is assumed that most rapidly proliferating cells in the population are also the largest cells in the population (Fig. 13, top row). This would account for the observations that within a given lymphoma sample, the subpopulation with the largest G_1 Coulter volume has the largest fraction of S associated with it, and lymphomas that consist predominantly of large cells have both large G_1 cells and high S fractions. (*b*) All cells increase in size as they progress through the cell cycle. Cells that remain members of the same cell cycle time class from one generation to the next will, on the average, double in size between divisions, and halve their size at mitosis. To account for the observed relation between mean G_1 Coulter volume and the fraction of cells in S among subpopulations within individual samples, we assume that cells that undergo growth retardation, i.e., lengthening of cell cycle time, do not quite double in size between divisions. Their G_1 progeny will be smaller than G_1 cells that did not undergo growth retardation. (*c*) To account for the heterogeneity in G_1 Coulter volumes that is observed in each sample, we assume that cells that have spiralled into a longer cell cycle time class can either remain members of that cell cycle time class or they can spiral into still longer cycles. Although it is possible for some slowly proliferating cells to shorten their cell cycle time under steady-state growth conditions, the net flow of cells must be from shorter to

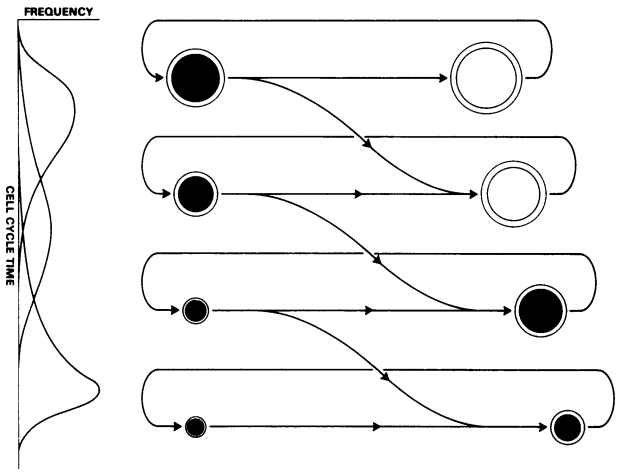

FIGURE 13 The schematic representation of a model for the kinetic and cytomorphologic heterogeneity in the lymphomas. For discussion, see text.

longer cycles. Otherwise, the most rapidly proliferating cells would quickly overgrow all others, and every lymphoma would consist of large cells only. (*d*) The overall distribution of cell sizes and the overall fraction of cells in S in a given sample would depend to a large extent on the relative abundance of rapidly proliferating and slowly proliferating cells, particularly in the B cell lymphomas. B cell lymphomas in which slowly proliferating cells predominate would consist mainly of small cells. Because the portions of long cycles that are devoted to active DNA synthesis would be relatively small, few of these slowly proliferating cells are likely to be engaged in active DNA synthesis at any given time, and nearly all of the cells would have the Coulter volumes and DNA content of small G_1 cells; that is, these cells would exhibit both morphologic features and DNA content distributions that are characteristic of mature lymphocytes. If there is a separate and distinct G_0 state, then the G_0 cells are likely to be found in this cell subpopulation and would have to be distinguished from it.

In the T cell lymphomas, although the relationship between proliferative rate and G_1 cell size is preserved within individual samples, it would appear that there are other factors in addition to proliferative rate that affect the range of cell sizes that might be observed within and among different samples.

The model shown in Fig. 13 is valid only for populations that are homogeneous with respect to ploidy. In diploid-aneuploid mixtures, the model can be applied to each component separately.

The model is useful in that it organizes and integrates a variety of different and seemingly disparate observations. The model provides for both cell cycle position-dependent cell size correlations and proliferation rate-dependent correlations with G_1 cell size among tumors (Figs. 2 and 8), but assigns major importance to the latter (Fig. 8). At the same time, the model provides for a correlation between G_1 cell size and the fraction of cells in S among different samples (Fig. 9) and among cell subpopulations within individual samples (Figs. 11 and 12).

The model also provides a rational framework, based on cell proliferative behavior, for the histopathologic classification of the lymphomas, particularly those of the B-cell series. A rapidly proliferating large B-cell lymphoma with a high S fraction (upper cell cycle time distribution curve, left panel, Fig. 13) might be labeled an immunoblastic sarcoma according to the Lukes and Collins classification, or a histiocytic lymphoma in the Rappaport classification. A more slowly proliferating B cell lymphoma (middle cell cycle time distribution, left panel, Fig. 13) might be labeled a small cleaved cell lymphoma in the Lukes and Collins classification or a poorly differentiated lymphoma in the Rappaport classification. The model focuses on the proliferative processes that underlie the diagnostic labels. It provides the conceptual tools for dealing with quantitative aspects of heterogeneity in growth behavior and cytomorphology within and among the lymphomas.

This model also has its limitations. Braylan et al. (23) have reported that Burkitt lymphomas exhibit much higher S fractions than histiocytic lymphomas, but lower modal Coulter volumes and/or coefficients of variation of cell size. Thus, one cannot simply equate large cell size with rapid cell proliferation and small cell size with slow proliferation. Other cytomorphologic features, such as nuclear cleavage and nuclear convolution may be related to cell proliferative rate in ways that are not accounted for by the present model. The relations between tissue microarchitecture (e.g., nodularity vs. diffuseness, the presence or absence of sclerosis) and population proliferation characteristics are also not considered within the context of the cytomorphologic model.

Finally, the model shown in Fig. 13 is most appropriate for describing the proliferative behavior of established lymphomas under stable steady-state or slowly changing growth conditions. Under these conditions, the growth retardation of rapidly proliferating cells would account for the fact that kinetic and morphologic heterogeneity are maintained in individual tumors over the course of time.

The process of malignant transformation itself, and transformations over the long term from small cell to large cell lymphomas may be described more aptly by models involving clonal selection and clonal evolution (46, 47). In recent cytogenetic studies employing chromosomal banding techniques, the prevalence of karyotypic abnormalities in the lymphomas has been found to approach 100% (48–55).

Modal chromosome numbers commonly fall within the near diploid range, especially in the small cell

lymphomas (54). In all likelihood then, the cases of B and T cell lymphoma that we reported as diploid by flow cytometry (Table I) contained cytogenetically abnormal stem lines that could not be distinguished from diploid reference cells in our studies. Furthermore, since all of the samples that we studied consisted of tissue that was largely replaced by neoplastic cells by histologic criteria, it is likely that these cytogenetically abnormal cells were a prominent cell component. The same considerations apply to the seemingly diploid cell component in the samples that exhibited mixed ploidy in our study. Presumably, many of these "diploid" cells were minimally aneuploid as well.

Although flow cytometry is not as sensitive as chromosomal banding methods in detecting cytogenetic abnormalities, it does offer certain other advantages. When populations of mixed ploidy can be demonstrated by flow cytometry, and when the component populations are separable, it is possible to determine the proportion of each component in the mixture and to study its proliferative characteristics separately.

Our findings indicate that the large cell lymphomas often consist of mixtures which include populations of large markedly aneuploid cells with high proliferative rates. These cell populations constitute a larger fraction of the total sample in the large cell lymphomas than in the small cell lymphomas. It is common to observe the transformation of small cell lymphomas to large cell lymphomas in individual patients over the course of time (56–58). These observations can be explained either in terms of clonal selection or on the basis of clonal evolution, whereby an underlying acquired genetic variability permits the sequential selection of progressively more malignant cell sublines (46, 47). Clonal evolution has been demonstrated in other hematologic malignancies (59–61). It may be possible to study these processes in detail in future studies of the lymphomas by carrying out serial dual parameter flow cytometry studies in conjunction with cytogenetic studies in individual patients.

REFERENCES

1. Taylor, C. R. 1978. Classification of lymphoma. *Arch. Pathol. Lab. Med.* **102:** 549–554.
2. Jones, S. E., Z. Fuks, M. Bull, M. E. Kadin, R. F. Dorfman, H. S. Kaplan, S. A. Rosenberg, and H. Kim. 1973. Non-Hodgkin's lymphomas. IV. Clinicopathologic correlation in 405 cases. *Cancer (Phila.).* **31:** 806–823.
3. Schein, P. S., B. A. Chabner, G. P. Canellos, R. C. Young, C. W. Berard, and V. T. DeVita. 1974. Potential for prolonged disease-free survival following combination chemotherapy of non-Hodgkin's lymphoma. *Blood.* **43:** 187–189.
4. Anderson, T., R. A. Bender, R. I. Fisher, V. T. DeVita, B. A. Chabner, C. W. Berard, L. Norton, and R. C. Young. 1977. Combination chemotherapy in non-Hodgkin's lymphoma: results of long-term follow-up. *Cancer Treat. Rep.* **61:** 1057–1066.
5. Cadman, E., L. Farber, D. Berd, and J. Bertino. 1977. Combination therapy for diffuse histiocytic lymphoma that includes antimetabolites. *Cancer Treat. Rep.* **61:** 1109–1116.
6. DeVita, V. T., G. P. Canellos, B. Chabner, P. Schein, S. P. Hubbard, and R. C. Young. 1975. Advanced diffuse histiocytic lymphoma, a potentially curable disease. *Lancet.* **I:** 248–250.
7. Portlock, C. S., and S. A. Rosenberg. 1979. No initial therapy for Stage III and IV non-Hodgkin's lymphomas of favorable histologic types. *Ann. Intern. Med.* **90:** 10–13.
8. Ishii, Y., M. Mori, and T. Onoe. 1972. Studies on the germinal center. IV. Autoradiographic study of lymph node germinal centers in relation to zonal differentiation. *J. Reticuloendothel. Soc.* **11:** 383–393.
9. Miller, S. C., and D. G. Osmond. 1973. The proliferation of lymphoid cells in guinea pig bone marrow. *Cell Tissue Kinet.* **6:** 259–269.
10. Osmond, D. G., and N. B. Everett. 1964. Radioautographic studies of bone marrow lymphocytes *in vivo* and in diffusion chamber cultures. *Blood.* **23:** 1–17.
11. Yoshida, Y., and D. G. Osmond. 1971. Identity and proliferation of small lymphocyte precursors in cultures of lymphocyte-rich fractions of guinea pig marrow. *Blood.* **37:** 73–86.
12. Lukes, R. J., J. W. Parker, C. R. Taylor, B. H. Tindle, A. D. Cramer, and T. L. Lincoln. 1978. Immunologic approach to non-Hodgkin's lymphomas and related leukemias. Analysis of the results of multiparameter studies of 425 cases. *Semin. Hematol.* **15:** 322–351.
13. Shackney, S. E., B. W. Erickson, and K. S. Skramstad. 1979. The T-lymphocyte as a diploid reference standard for flow cytometry. *Cancer Res.* **39:** 4418–4422.
14. Lukes, R. J., and R. D. Collins. 1974. Immunologic characterization of human malignant lymphomas. *Cancer (Phila.).* **34:** 1488–1503.
15. Rappaport, H. 1966. Tumors of the Hematopoietic System. Atlas of Tumor Pathology, Sec. 3, fasc. 8. Washington, D. C., Armed Forces Inst. of Pathology.
16. Salzman, G. C., R. D. Hiebert, and J. M. Crowell. 1978. Data acquisition and display for a high-speed cell sorter. *Comput. Biomed. Res.* **11:** 77–88.
17. Jett, J. H. 1978. Mathematical analysis of DNA histograms from asynchronous and synchronous cell populations. *In* Proceedings of the 3rd International Symposium on Pulse Cytophotometry. D. Lutz, editor. European Press, Ghent, Belgium. 93–102.
18. Alabaster, O., D. L. Glaubiger, V. T. Hamilton, S. A. Bentley, S. E. Shackney, K. S. Skramstad, and R. F. Chen. 1980. Electrolytic degradation of DNA fluorochromes during flow cytometric measurement of electronic cell volume. *J. Histochem. Cytochem.* **28:** 330–334.
19. Shackney, S. E. 1977. DNA content distributions, cell kinetics, and cell morphology: theoretical considerations, experimental correlations, and clinical implications. *In* Growth Kinetics and Biochemical Regulation of Normal and Malignant Cells. B. Drewinko and R. M. Humphrey, editors. The Williams & Wilkins Company, Baltimore. 391–409.
20. Shackney, S. E., and K. S. Skramstad. 1979. A dynamic interpretation of multiparameter studies in the lymphomas. *Am. J. Clin. Pathol.* **72:** 756–764.
21. Barlogie, B., W. Hittelman, G. Spitzer, J. M. Trujillo, J. S. Hart, L. Smallwood, and B. Drewinko. 1977. Correlation of DNA distribution abnormalities with cytogenetic findings in human adult leukemia and lymphoma. *Cancer Res.* **37:** 4400–4407.
22. Diamond, L. W., and R. C. Braylan. 1980. Flow analysis of

DNA content and cell size in non-Hodgkin's lymphoma. *Cancer Res.* **40:** 703–712.
23. Braylan, R. C., B. J. Fowlkes, E. S. Jaffe, S. K. Sanders, C. W. Berard, and C. J. Herman. 1978. Cell volumes and DNA distributions of normal and neoplastic human lymphoid cells. *Cancer (Phila.)* **41:** 201–209.
24. Millikin, P. D. 1966. Anatomy of germinal centers in human lymphoid tissue. *Arch. Pathol.* **82:** 499–505.
25. Hanna, M. G., Jr. 1964. An autoradiographic study of the germinal center in spleen white pulp during early intervals of the immune response. *Lab. Invest.* **13:** 95–104.
26. Weinbeck, J. 1938. Die granulopoese des kindlichen knochenmarkes und ihre reaktion auf infectionen. *Beitr. Pathol. Anat. Allg. Pathol.* **101:** 268–300.
27. Lennert, K. 1952. Zur praxis der pathologich-anatomichen knochenmarksuntersuchung. *Frankf. Z. Pathol.* **63:** 267–299.
28. Cronkite, E. P., V. P. Bond, T. M. Fleidner, and S. A. Killmann. 1960. The use of tritiated thymidine in the study of haemopoietic cell proliferation. *In* Cell Production and Its Regulation, Ciba Foundation Symposium on Haemopoiesis. M. O'Connor and G. E. W. Wolstensholme, editors. Little, Brown, & Co., Boston. 70–92.
29. Shackney, S. E., S. S. Ford, and A. B. Wittig. 1975. Kinetic microarchitectural correlations in the bone marrow of the mouse. *Cell Tissue Kinet.* **8:** 505–516.
30. Borum, K. 1968. Pattern of cell production and cell migration in mouse thymus studied by autoradiography. *Scand. J. Haematol.* **5:** 339–352.
31. Borum, K. 1973. Cell kinetics in mouse thymus studied by simultaneous use of ^{3}H-thymidine and colchicine. *Cell Tissue Kinet.* **6:** 545–552.
32. Ford, J. K., and R. W. Young. 1963. Cell proliferation and displacement in the adrenal cortex of young rats injected with tritiated thymidine. *Anat. Rec.* **146:** 125–133.
33. Grisham, J. W. 1962. A morphologic study of deoxyribonucleic acid synthesis and cell proliferation in regenerating rat liver; autoradiography with thymidine-H^3. *Cancer Res.* **22:** 842–849.
34. Iversen, O. H., R. Bjerknes, and F. Devik. 1968. Kinetics of cell renewal, cell migration, and cell loss in the hairless mouse dorsal epidermis. *Cell Tissue Kinet.* **1:** 351–367.
35. Leblond, C. P., R. C. Greulich, and J. P. M. Periera. 1964. Relationship of cell formation and cell migration in the renewal of stratified squamous epithelia. *Adv. Biol. Skin.* **5:** 39–67.
36. Quastler, H., and F. G. Sherman. 1959. Cell population kinetics in the intestinal epithelium of the mouse. *Exp. Cell Res.* **17:** 420–438.
37. Wright, N. A. 1971. Cell proliferation in the prepubertal male rat adrenal cortex: an autoradiographic study. *J. Endocrinol.* **49:** 599–609.
38. Tannock, I. F. 1968. The relation between cell proliferation and the vascular system in a transplanted mouse mammary tumor. *Br. J. Cancer.* **22:** 258–273.
39. Clarkson, B. D., J. Fried, Y. Sakai, A. Strife, K. Ota, and T. Ohkita. 1970. Studies of cellular proliferation in human leukemia. III. Behavior of leukemic cells in three adults with acute leukemia given continuous infusions of ^{3}H-thymidine. *Cancer (Phila.).* **25:** 1237–1260.
40. Clarkson, B. D., Y. Sakai, T. Kimura, T. Ohkita, and J. Fried. 1968. Studies of cellular proliferation in human leukemia. II. Variability in rates of growth and cellular differentiation in acute myelomonocytic leukemia and effects of treatment. *In* The Proliferation and Spread of Neoplastic Cells. The Williams & Wilkins Company, Baltimore. 295–330.
41. Gavosto, F., A. Pileri, C. Bachi, and L. Pegoraro. 1964. Proliferation and maturation defect in acute leukemia cells. *Nature (Lond.).* **203:** 92–94.
42. Gavosto, F., A. Pileri, V. Gabutti, and P. Masera. 1967. Non-self-maintaining kinetics of proliferating blasts in human acute leukemia. *Nature (Lond.).* **216:** 188–189.
43. Saunders, E. F., B. C. Lampkin, and A. M. Mauer. 1967. Variation of proliferative activity in leukemic cell populations of patients with acute leukemia. *J. Clin. Invest.* **46:** 1356–1363.
44. Metcalf, D., and M. Wiadrowski. 1966. Autoradiographic analysis of lymphocyte proliferation in the thymus and in thymic lymphoma tissue. *Cancer Res.* **26:** 483–491.
45. Omine, M., G. P. Sarna, and S. Perry. 1973. Composition of leukemic cell populations in AKR leukemia and effects of chemotherapy. *Eur. J. Cancer.* **9:** 557–565.
46. Clarkson, B. D., and S. I. Rubinow. 1977. Growth kinetics in human leukemia. *In* Growth Kinetics and Biochemical Regulation of Normal and Malignant Cells. B. Drewinko and R. M. Humphrey, editors. The Williams & Wilkins Company, Baltimore. 591–628.
47. Nowell, P. C. 1976. The clonal evolution of tumor cell populations. *Science (Wash. D. C.).* **194:** 23–28.
48. Erkman-Balis, B., and H. Rappaport. 1974. Cytogenetic studies in mycosis fungoides. *Cancer (Phila.).* **34:** 626–633.
49. Fleischman, E. W., and E. L. Prirogina. 1977. Karyotype peculiarities of malignant lymphomas. *Hum. Genet.* **35:** 269–279.
50. Fukuhara, S., and J. D. Rowley. 1978. Chromosome 14 translocations in non-Burkitt lymphomas. *Int. J. Cancer.* **22:** 14–21.
51. Fukuhara, S., J. D. Rowley, D. Variakojis, and H. M. Golomb. 1979. Chromosome abnormalities in poorly differentiated lymphomas. *Cancer Res.* **39:** 3119–3128.
52. Fukuhara, S., J. D. Rowley, D. Variakojis, and D. L. Sweet. 1978. Banding studies on chromosomes in diffuse "histiocytic" lymphomas: correlation of 14q+ marker chromosome with cytology. *Blood.* **52:** 989–1002.
53. Mark, J., C. Ekedahl, and A. Hagman. 1977. Origin of the translocated segment of the 14q+ marker in non-Burkitt lymphomas. *Hum. Genet.* **36:** 277–282.
54. Reeves, B. R. 1973. Cytogenetics of malignant lymphomas. *Hum. Genet.* **20:** 231–250.
55. Whang-Peng, J., M. Lutzner, R. Edelson, and T. Knutsen. 1976. Cytogenetic studies and clinical implications in patients with Sezary syndrome. *Cancer (Phila.).* **38:** 861–867.
56. Cullen, M. H., T. A. Lister, R. L. Brearley, W. S. Shand, and A. G. Stansfeld. 1979. Histological transformation of non-Hodgkin's lymphoma. A prospective study. *Cancer (Phila.).* **44:** 645–651.
57. Katayama, I., L. Ceccacci, A. F. Valu, and E. O. Horne. 1977. Histiocytic lymphoma with sclerosis arising from a nodular lymphoma with a special stromal reaction. An ultrastructural study. *Cancer (Phila.).* **40:** 2203–2208.
58. Risdall, R., R. T. Hoppe, and R. Warnke. 1979. Non-Hodgkin's lymphoma. A study of the evolution of the disease based upon 92 autopsied cases. *Cancer (Phila.).* **44:** 529–542.
59. Oshimura, M., A. I. Freeman, and A. A. Sandberg. 1977. Chromosomes and the causation of human cancer and leukemia. XXVI. Banding studies in acute lymphoblastic leukemia (ALL). *Cancer (Phila.).* **40:** 1161–1172.
60. Testa, J. R., U. Mintz, J. D. Rowley, J. W. Vardiman, and H. M. Golomb. 1979. Evolution of karyotypes in acute nonlymphocytic leukemia. *Cancer Res.* **39:** 3619–3627.
61. Zeulzer, W. W., S. Inoue, R. I. Thompson, and M. J. Ottenbreit. 1976. Long-term cytogenetic studies in acute leukemia of children: the nature of relapse. *Am. J. Hematol.* **1:** 143–190.